Absolute Negative Conductivity and Spontaneous Current Generation in Semiconductor Superlattices with Hot Electrons

Ethan H. Cannon,[1] Feodor V. Kusmartsev,[2] Kirill N. Alekseev,[3] and David K. Campbell[1]

[1]*Department of Physics, University of Illinois at Urbana-Champaign, 1110 West Green Street, Urbana, Illinois 61801*

[2]*Department of Physics, Loughborough University, Loughborough LE11 3TU, United Kingdom*

[3]*Department of Physical Sciences, University of Oulu, Oulu FIN-90014, Finland*

(Received 7 October 1999)

We study transport through a semiconductor superlattice with an electric field parallel to and a magnetic field perpendicular to the growth axis. Using a semiclassical balance equation model with elastic and inelastic scattering, we find that (1) the current-voltage characteristic becomes multistable in a large magnetic field and (2) "hot" electrons display novel features in their current-voltage characteristics, including absolute negative conductivity and a spontaneous dc current at zero bias. We discuss experimental situations providing hot electrons to observe these effects.

PACS numbers: 73.20.Dx, 72.80.Ey, 73.40.Gk

Semiconductor superlattices (SSLs) are excellent systems for exploring nonlinear transport effects, since their long spatial periodicity implies that SSLs have small Brillouin zones and very narrow "minibands" [1]. Applied fields accelerate Bloch electrons in a band according to $\dot{\mathbf{k}} = -(e/\hbar)[\mathbf{E} + (\mathbf{v} \times \mathbf{B})/c]$, with momentum $\mathbf{k}$, charge $-e$, electric field $\mathbf{E}$, magnetic field $\mathbf{B}$, electron velocity $\mathbf{v}$, and speed of light c. In SSLs, both the velocity and effective mass depend on the momentum; the effective mass is negative above the band's inflection point, corresponding to the fact that electrons slow down to zero velocity at the Brillouin zone edge. The acceleration of the external fields is balanced by scattering processes that limit the momentum of electrons. In clean SSLs with modest fields, electrons can reach the negative effective mass (NEM) portion of the miniband before scattering. For an electric field oriented along the growth axis, the current-voltage characteristic exhibits a peak followed by negative differential conductivity (NDC) when a significant fraction of electrons explore the NEM region of the miniband [1]; with an additional magnetic field perpendicular to the growth axis, NDC occurs at a *larger* bias because the magnetic field impedes the increase of momentum along the growth axis [2].

We study electron transport through a single miniband, spatially homogeneous SSL with a constant magnetic field, B, in the x direction and an electric field, E, along the growth axis (the z direction). We assume a tight-binding dispersion relation, $\epsilon(\mathbf{k}) = \hbar^2(k_x^2 + k_y^2)/2m^* + \Delta/2[1 - \cos(k_z a)]$, where ϵ is the energy of an electron with momentum $\mathbf{k}$, m^* is the effective mass within the plane of the quantum wells that form the SSL, Δ is the miniband width, and a the SSL period.

Generalizing the approach of [3] to include the effects of the magnetic field, we obtain the balance equations [4]

$$\dot{V}_y = -eBV_z/m^*c - \gamma_{vy}V_y\,, \tag{1}$$

$$\dot{V}_z = -e[E - BV_y/c]/m(\varepsilon_z) - \gamma_{vz}V_z\,, \tag{2}$$

$$\dot{\varepsilon}_z = -eEV_z + eBV_y/cV_z - \gamma_\varepsilon[\varepsilon_z - \varepsilon_{eq,z}]. \tag{3}$$

The average electron velocity, $\mathbf{V} = (V_y, V_z)$, is obtained by integrating the distribution function satisfying the Boltzmann transport equation (BTE) over the Brillouin zone; γ_{vy} and γ_{vz} are relaxation rates for the corresponding components of $\mathbf{V}$ following from elastic impurity, interface roughness and disorder scattering, and inelastic phonon scattering. It is convenient to separate the energy of the electrons into parts associated with longitudinal and transverse motion; ε_z is the average energy of motion along the growth axis with equilibrium value $\varepsilon_{eq,z}$, and γ_ε represents its relaxation rate due mainly to inelastic phonon scattering (elastic scattering that reduces the energy of motion along the SSL growth axis and increases the transverse energy also contributes). The balance equations contain an effective mass term dependent on ε_z, $m(\varepsilon_z) = m_0/(1 - 2\varepsilon_z/\Delta)$, which follows from the momentum dependence of the effective mass tensor, and $m_0 = 2\hbar^2/\Delta a^2$ is the effective mass at the bottom of the SSL miniband. The transverse energy does not enter the balance equations because of the constant effective mass for this motion. While the magnetic field does not change the total electron energy, it does transfer energy between transverse motion and ε_z; hence Eq. (3) contains the magnetic field-dependent term.

Intuitively, we understand the balance equations as describing an "average" electron whose velocity changes according to $\dot{\mathbf{V}} = \mathbf{F}/\mathbf{m}(\varepsilon)$: $\mathbf{F}$ represents electric, magnetic, and damping forces. The mass tensor $\mathbf{m}(\varepsilon)$ is diagonal and m_{zz} depends on the energy of motion in the z direction; this energy component evolves according to $\dot{\varepsilon}_z = F_z V_z - P_{\text{damp}}$. Inelastic scattering to the average energy $\varepsilon_{eq,z}$ (which may not be the bottom of the miniband) leads to the damping term, P_{damp}. This intuitive picture should not obscure that our balance equations have been derived from the full BTE. Recent experimental and theoretical studies have shown that BTE-based semiclassical models are quite accurate when the energy drop per SSL period

 0031-9007/00/85(6)/1302(4)$15.00

from the electric field, eEa, remains less than the miniband width, Δ [5]; hence semiclassical models work well to suggest new directions for experiments and more detailed quantum mechanical models. Equivalently, this condition states that the electric field-induced Bloch oscillation frequency must be less than the miniband width; similarly, we expect the semiclassical model to apply when the miniband width exceeds the frequency of linear cyclotron oscillations, $\Delta > \hbar eB/(m_0 m^*)^{1/2}$. Larger magnetic fields necessitate a quantum model which includes the modification of the eigenfunctions and eigenenergies with magnetic field [6]. Miniband transport also requires $\Delta > \hbar\gamma$. Consider SSL parameters from the recent experiment [7]: $\gamma_{vy} = \gamma_{vz} = \gamma_\varepsilon = 10^{12}\ \mathrm{s}^{-1}$, $\Delta = 22$ meV, and $a = 90$ Å; the conditions $\hbar\omega_B < \Delta$ and $\hbar eB/(m_0 m^*)^{1/2} < \Delta$ are satisfied for electric fields less than 24 kV/cm and magnetic fields less than 14 T.

For numerical work, we use the scalings $v_y = \sqrt{m_0 m^*}\, a/\hbar V_y$, $v_z = m_0 a/\hbar V_z$, $w = (\varepsilon_z - \Delta/2)/(\Delta/2)$, $w_0 = (\varepsilon_{eq,z} - \Delta/2)/(\Delta/2)$, $\mathcal{B} = eB/\sqrt{m^* m_0}\, c$, and $\omega_B = eEa/\hbar$ (the Bloch frequency of the electric field). The average electron energy is scaled such that -1 $(+1)$ corresponds to the bottom (top) of the miniband. In these scaled variables, the balance equations read

$$\dot{v}_y = -\mathcal{B} v_z - \gamma_{vy} v_y\,, \tag{4}$$

$$\dot{v}_z = \omega_B w - \mathcal{B} v_y w - \gamma_{vz} v_z\,, \tag{5}$$

$$\dot{w} = -\omega_B v_z + \mathcal{B} v_y v_z - \gamma_\varepsilon (w - w_0)\,. \tag{6}$$

The current across the SSL $I = -eNA(\Delta a/2\hbar) v_{z,ss}$, where N is the carrier concentration, A the cross-sectional area, and $v_{z,ss}$ the steady-state solution to Eq. (5). Setting the time derivatives in Eqs. (4)–(6) to zero, we obtain the following equation relating the SSL current to the bias: $C^2 v_{z,ss}^3 + 2C\omega_B v_{z,ss}^2 + [\gamma_{vz}\gamma_\varepsilon + \omega_B^2 - \gamma_\varepsilon w_0 C] v_{z,ss} - \gamma_\varepsilon w_0 \omega_B = 0$, where $C = \mathcal{B}^2/\gamma_{vy}$. This cubic equation implies there may be up to three steady-state current values for a given bias [8].

In Fig. 1, we plot $-v_{z,ss}$, which is proportional to the current, as a function of voltage, ω_B, for three magnetic fields. With no magnetic field (Fig. 1a), the current exhibits a peak followed by NDC and satisfies the well-known expression $v_{z,ss} = (-w_0/\gamma_{vz})\omega_B/(1 + \omega_B^2/\gamma_{vz}\gamma_\varepsilon)$ [9]. With a magnetic field, the current reaches its maximum value at a larger electric field (Fig. 1b); this has been observed experimentally and is well understood [2]. For a larger magnetic field (Fig. 1c), the balance equations predict a region of multistability with three possible currents. This multistability occurs for $\omega_B/\gamma_{vz} \approx 7$–$8$ and, for wide miniband SSLs with low scattering, does not contradict the constraints of our semiclassical model, i.e., $\hbar\omega_B < \Delta$ and $\hbar\gamma_{vz} < \Delta$. For the low damping rates obtained in [7], $\Delta/\hbar\gamma_{vz} \approx 33$, so $\Delta/\hbar\omega_B \approx 4$ at the onset of multistability (in unscaled units, $\omega_B = 8\gamma_{vz}$ for an electric field of 6 kV/cm). The magnetic field in Fig. 1c also falls within the bounds of the semiclassical model: when $C = 15\gamma_{vz}$ (a field of 1.7 T), the miniband width is about 8.5 times the linear cyclotron frequency, $\mathcal{B}$.

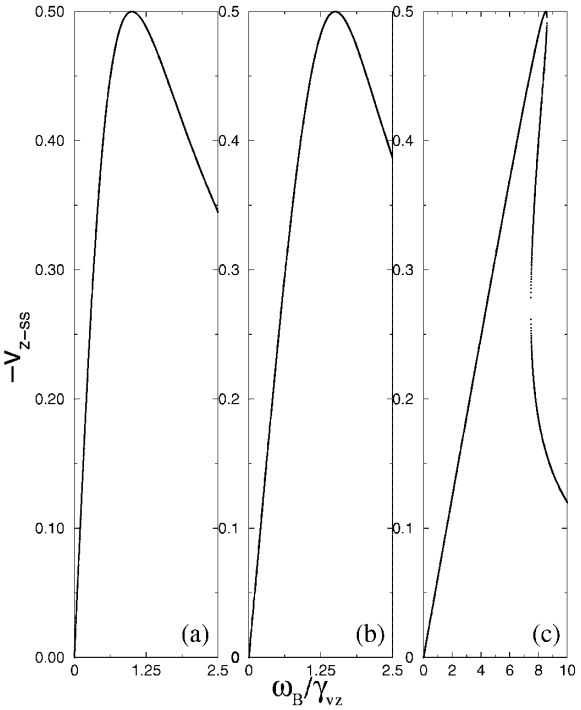

FIG. 1. Current-voltage characteristic with $\gamma_{vz} = \gamma_\varepsilon$ and $w_0 = -1$ for no magnetic field, $C = 0$ (a), a small magnetic field, $C = \gamma_{vz}$ (b), and a large magnetic field, $C = 15\gamma_{vz}$ (c).

We now consider "hot" electrons, where the electron distribution is highly nonthermal, even without the applied fields. The electrons do not have time to relax to the bottom of the miniband before leaving the SSL. We can effectively describe these hot carriers as relaxing to the top half of the miniband, i.e., as having $w_0 > 0$. This may happen in a very clean SSL at very low temperatures, when the inelastic mean free path is comparable with the SSL size. The hot electrons may be obtained by injection [7,10] or by optical excitation. Below we will discuss how to achieve this situation experimentally. For zero or small magnetic fields (Fig. 2a), absolute negative conductance (ANC) occurs as the current flows in the opposite direction as the applied bias. In larger magnetic fields (Fig. 2b), a region of multistability appears around zero bias; the zero current solution becomes unstable as soon as the nonzero current solutions emerge. *In other words, the SSL will spontaneously develop a current at zero bias.* The three possible zero-bias, steady-state velocities are $v_{z,ss} = 0, \pm(\frac{\gamma_\varepsilon w_0 C - \gamma_{vz}\gamma_\varepsilon}{C^2})^{1/2}$, so a spontaneous current will appear when $w_0 C > \gamma_{vz}$ (i.e., $w_0 \mathcal{B}^2/\gamma_{vy} > \gamma_{vz}$). Since C and γ_{vz} are always positive, this requires that w_0 be positive; neither thermal effects nor doping can fulfill the necessary condition for a zero-bias current: hot electrons are required. One clearly needs energy to create the spontaneous current, and hot electrons supply this

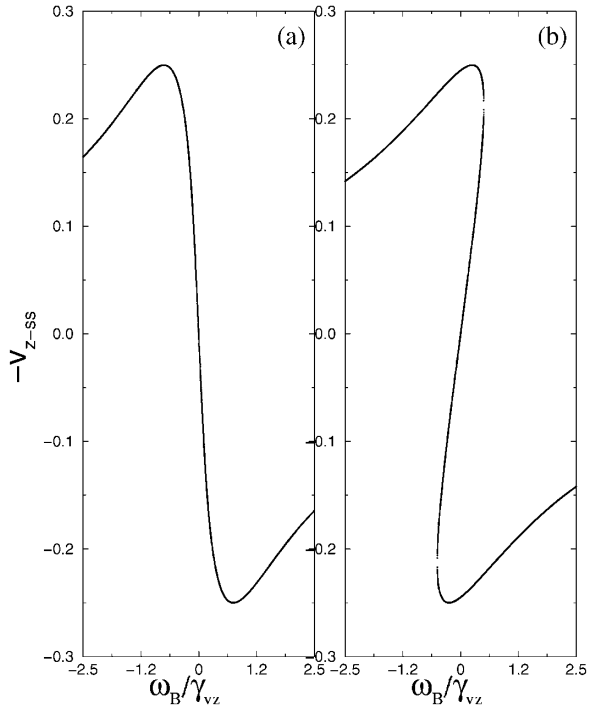

FIG. 2. Current-voltage characteristic for hot electrons, $w_0 = 0.5$ with $\gamma_{vz} = \gamma_\varepsilon$ in a small magnetic field, $C = \gamma_{vz}$ (a), and in a large magnetic field, $C = 5\gamma_{vz}$ (b).

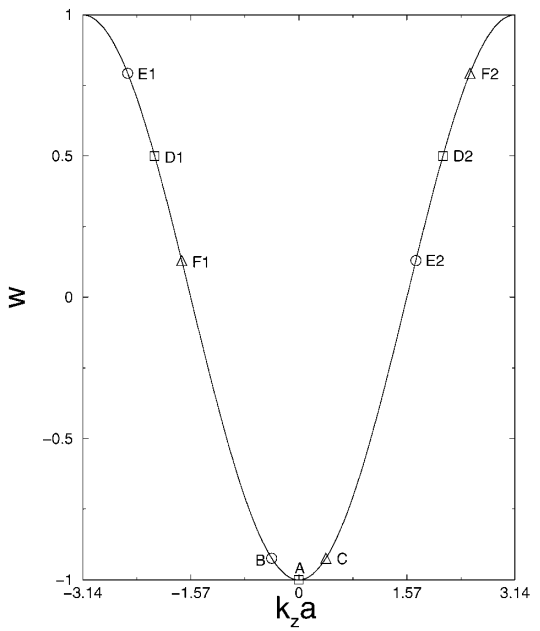

FIG. 3. Miniband structure; labeled points are described in text.

energy. Moreover, the condition for a spontaneous current does not violate our assumption of semiclassical transport. The SSL generates a current when $\mathcal{B} \simeq \gamma$, but the condition $\Delta > \hbar\mathcal{B}$ can be satisfied since $\Delta > \hbar\gamma$. Consider again the parameters of Ref. [7]: for $w_0 = 0.5$, a spontaneous current occurs for $\mathcal{B} \approx 1.4\gamma_{vz}$ ($B = 0.6$ T), so that $\Delta \approx 23\hbar\mathcal{B}$.

Hot electrons lead to ANC and spontaneous current generation because of their NEM in the top half of the miniband. To understand the origin of ANC, consider a one-dimensional SSL with electrons at their equilibrium position at the bottom of the band, $w_0 = -1$, and no electric field; when a positive bias is applied, $\omega_B > 0$, the electrons move through the band according to $\dot{k}_z a = -\omega_B$ until they scatter. Elastic scattering conserves energy, sending an electron across the band in this one-dimensional case. Inelastic scattering changes the energy to w_0, i.e., $k_z = 0$. (Hot electrons inelastically scatter to $w_0 > 0$, possibly gaining energy.) In Fig. 3, the electric field accelerates the electrons from their equilibrium position at point A; inelastic scattering prevents many electrons from passing point B, so electrons are found mainly in the segment AB. Elastic scattering sends electrons into the segment AC, which contains fewer electrons than the segment AB. In this tight-binding miniband, the electron velocity is $\mathcal{V}(k_z) \equiv \hbar^{-1}\partial\epsilon/\partial k_z = (\Delta a/2\hbar)\sin(k_z a)$; because the segment AB has more electrons, there is a net negative velocity, or a positive current. For hot electrons with $w_0 > 0$, initially the points labeled $D1$ and $D2$ are occupied with equal numbers of electrons, and no current flows. Once applied, the electric field accelerates electrons such that they occupy the segments $D1E1$ and $D2E2$, as inelastic (nonenergy-conserving) scattering returns them to their quasiequilibrium energy at points $D1$ and $D2$; elastic scattering leads to a smaller number of electrons in the segments $D1F1$ and $D2F2$. The speed of electrons above the miniband inflection point decreases as the magnitude of their momentum approaches the Brillouin zone edge; thus the electrons in the segment $D2E2$ have a larger speed than those in $D1E1$. A positive net velocity or, in other words, a negative current results; this is the ANC shown in Fig. 2a.

An intuitive picture of the spontaneous current generation also follows from the SSL miniband structure. Consider a small, positive current fluctuation resulting from extra electrons at the initial energy $w_0 > 0$ (point $D2$ in Fig. 3). The momentum evolves according to $\dot{\mathbf{k}} = -(e/\hbar c)\mathcal{V} \times \mathbf{B}$; with $B_x > 0$, initially $\dot{k}_y > 0$, and $\dot{k}_z < 0$. In the magnetic field, the hot electrons move from point $D2$ towards $E2$. Approaching the miniband inflection point, the electrons speed up, and the current fluctuation grows. Eventually an electron will scatter inelastically to its quasiequilibrium initial position or elastically across the band. For magnetic field strength and scattering rates specified by the requirement $w_0\mathcal{B}^2 > \gamma_{vy}\gamma_{vz}$, the initial current fluctuation associated with the hot electrons will increase, the zero current state will be unstable to such small fluctuations, and the SSL will develop a spontaneous current.

Experimentally, it is possible to obtain hot electrons with $w_0 > 0$ by injecting electrons into the NEM portion of

the miniband, as was described in Refs. [7,10]. In the steady state, a continuous stream of energetic electrons replaces the carriers that tunnel out of the finite SSL, acting as the constant energy source requisite for spontaneous current generation. In the balance equation formalism, hot electrons are described by a positive average energy, $w_0 > 0$, and act as an energy source in Eq. (6); without applied fields, hot electrons provide energy at the same rate γ_ε dissipates energy, hence $w = w_0$. Since w_0 is the average energy of the steady-state, zero-field electron distribution—including the width of the injection wave packet—this distribution must be peaked in the upper half of the miniband to yield $w_0 > 0$. This distribution shows that hot electrons provide the energy for the zero-bias current, and no basic physical laws are violated. Experiments measure the current transmitted through the SSL as a function of the incident energy of the injected carriers [7,10]. For this geometry, phonon scattering is negligible at low temperatures, and elastic interface roughness scattering is the main mechanism to decrease the energy of motion along the growth axis. To observe the hot electron effects we predict, the experiment must first be performed with a small electric field but no magnetic field; it must then be repeated with a magnetic field in the plane of the quantum well. Spontaneous current generation can occur for an electron wave packet incident at the top half of the miniband, and will lead to an increase of the transmitted current for appropriate energies (the small electric field merely selects the sign of the spontaneous current). ANC can be observed by measuring the transmitted current in both positive and negative electric fields; a positive (negative) electric field reduces (increases) the current. Finally, for the experiments we propose on undoped SSLs with low injection rates, electron-electron interactions are negligible; larger carrier concentrations necessitate a self-consistent theory to include carrier inhomogeneities and accumulation.

In summary, we have described new physical effects—current flow opposite to the direction of the applied electric bias and spontaneous current generation—in an SSL with a transverse magnetic field and nonequilibrium electron excitations, and we have suggested how they might be observed in experiments. We hope our experimental colleagues will search for these effects. Finally, we mention the discussion of similar effects (absolute negative conductivity, multistability, and spontaneous current generation) in a very different physical situation, i.e., an ac electric field and no magnetic field [11].

We are grateful to Lawrence Eaves and Erich Gornik for stimulating discussions. F. V. K. thanks the Department of Physics at the University of Illinois at Urbana-Champaign for its hospitality. This work was partially supported by NATO Linkage Grant No. NATO LG 931602 and RFBR. E. H. C. acknowledges support under NSF GER93-54978.

[1] L. Esaki and R. Tsu, IBM J. Res. Dev. **14**, 61 (1970).
[2] F. Aristone *et al.,* Appl. Phys. Lett. **67**, 2916 (1995); L. Canali *et al.,* Superlattices Microstruct. **22**, 155 (1997); B. Sun *et al.,* Phys. Rev. B **60**, 8866 (1999).
[3] A. A. Ignatov and V. I. Shashkin, Phys. Lett. **94A**, 169 (1983).
[4] E. H. Cannon, K. N. Alekseev, D. K. Campbell, and F. V. Kusmartsev (unpublished).
[5] A. Sibille *et al.,* Superlattices Microstruct. **13**, 247 (1993); A. Wacker and A.-P. Jauho, Phys. Rev. Lett. **80**, 369 (1998); A. Wacker *et al.,* Phys. Rev. Lett. **83**, 836 (1999).
[6] J. A. Simmons *et al.,* Phys. Rev. Lett. **73**, 2256 (1994); T. S. Lay, X. Ying, and M. Shayegan, Phys. Rev. B **52**, R5511 (1995).
[7] C. Rauch *et al.,* Phys. Rev. Lett. **81**, 3495 (1998).
[8] É. M. Épshtein, Radiophys. Quantum Electron. (Consultant's Bureau) **22**, 259 (1979); Sov. Phys. Semicond. **25**, 216 (1991). These references discuss a similar effect: a multivalued Hall voltage for large current bias.
[9] A. A. Ignatov, E. P. Dodin, and V. I. Shashkin, Mod. Phys. Lett. **5B**, 1087 (1991).
[10] C. Rauch *et al.,* Appl. Phys. Lett. **70**, 649 (1997); C. Rauch *et al.,* Superlattices Microstruct. **25**, 47 (1999).
[11] A. A. Ignatov and Yu. A. Romanov, Phys. Status Solidi B **73**, 327 (1976); A. A. Ignatov *et al.,* Z. Phys. B **98**, 187 (1995); B. J. Keay *et al.,* Phys. Rev. Lett. **75**, 4102 (1995); G. Platero and R. Aguado, Appl. Phys. Lett. **70**, 3546 (1997); K. N. Alekseev *et al.,* Phys. Rev. Lett. **80**, 2669 (1998); R. Aguado and G. Platero, Phys. Rev. Lett. **81**, 4971 (1998); K. N. Alekseev, M. V. Erementchouk and F. V. Kusmartsev, Europhys. Lett. **47**, 595 (1999).